Liquid–Liquid Phase Separation in Polysulfone/Polyethersulfone/*N*-Methyl-2-Pyrrolidone/Water Quaternary System

KI-JUN BAIK,[1] JE YOUNG KIM,[2] HWAN KWANG LEE,[3] SUNG CHUL KIM[2]

[1] Planning Department, Daelim Industrial Co. Ltd., Yusung P.O. Box 116, Taejon 305-600, South Korea

[2] Center for Advanced Functional Polymers, Korea Advanced Institute of Science and Technology, 373-1, Kusung-Dong, Yusung-Gu, Taejon 305-701, South Korea

[3] Department of Industrial Chemistry, Chungwoon University, #29, Namjang-Ri, Hongsung-Eub, Hongsung-Gun, Chungnam 350-800, South Korea

Received 15 April 1998; accepted 5 October 1998

ABSTRACT: To construct a phase diagram of the polysulfone (PSF)/polyethersulfone (PES)/*N*-methyl-2-pyrrolidone (NMP)/water quaternary system, cloud point measurements were carried out by a titration method. The miscible region in the PSF/PES/NMP/water quaternary system was narrow compared to the PSF/NMP/water and PES/NMP/water ternary systems. The binary interaction parameters between PSF and PES were estimated by water sorption experiments. The calculated phase diagram based on the Flory–Huggins theory fit the experimental cloud points well. In addition to the usual polymer–liquid phase separation, polymer–polymer phase separation, which resulted in a PSF-rich phase and a PES-rich phase, was observed with the addition of a small amount of nonsolvent. The boundary separating these two modes of phase separation could be well described and predicted from the calculated phase diagrams with the estimated binary interaction parameters of the components. © 1999 John Wiley & Sons, Inc. J Appl Polym Sci 74: 2113–2123, 1999

Key words: liquid–liquid phase separation; polysulfone; polyethersulfone; quaternary system; Flory–Huggins theory

INTRODUCTION

The phase inversion method is widely used to prepare a variety of polymeric membranes for microfiltration to gas separation.[1] This process is based on the phenomenon of liquid–liquid phase separation in which a homogeneous polymer solution undergoes phase separation into a polymer-rich phase and a polymer-lean phase by the exchange of solvent and nonsolvent in a coagulation bath. The final morphology obtained by immersion precipitation strongly reflects the thermodynamics and kinetics of the system involved. The equilibrium thermodynamics of the ternary system of polymer/solvent/nonsolvent is very important to understand and predict membrane structure,[2–4] because the diffusion mechanism and kinetics of phase separation are dictated by the location and quench depth in the phase diagram. One has to also consider the combination of liquid–solid and liquid–liquid phase equilibria when a crystallizable polymer is used.[5–7]

Correspondence to: S. C. Kim (kimsc@sorak.kaist.ac.kr).
Contract grant sponsor: Daelim Industrial Co., Ltd.

Journal of Applied Polymer Science, Vol. 74, 2113–2123 (1999)
 CCC 0021-8995/99/092113-11

Polysulfone (PSF) and polyethersulfone (PES) are important as polymer membrane materials because of their chemical resistance, mechanical strength, thermal stability, and transport properties.[8,9] There are several reports on experimental phase diagrams in ternary mixtures of PSF/solvent/nonsolvent[10–14] and PES/ solvent/nonsolvent.[11,15] It was found for both systems that liquid–liquid phase separation was not accompanied by crystallization and a small amount of nonsolvent was required to achieve liquid demixing. This was mainly attributed to the hydrophobic characteristics of the polymer as indicated in the literature.[2,13] It would be interesting to investigate the solution thermodynamics when these two polymers are present because PES is slightly less hydrophobic than PSF.[9,11,16,17] There is also a chance to control the rheological properties of the casting solution by changing the blend ratio of PSF and PES, especially when a concentrated solution is needed.

This article deals with liquid–liquid phase separation in a quaternary solution of PSF/PES/*N*-methyl-2-pyrrolidone (NMP)/water. The objectives of this work were to obtain the cloud point curve for the quaternary system and to provide a sound thermodynamic foundation based on the Flory–Huggins theory. The importance and implication of liquid demixing in the quaternary system are discussed when two polymers are used.

THERMODYNAMICS OF QUATERNARY SYSTEMS

The Flory–Huggins lattice treatment[18,19] is used to describe the thermodynamics of the quaternary system because of its simplicity. It is assumed that only binary interactions are significant and interaction parameters are constant, although slightly concentration-dependent parameters were reported for the system studied in this work.[15,20] The Gibbs free energy of mixing (ΔG_m) in quaternary solutions is given by

$$\begin{aligned}\Delta G_m/RT = {} & n_1 \ln \phi_1 + n_2 \ln \phi_2 + n_3 \ln \phi_3 \\ & + n_4 \ln \phi_4 + g_{12} n_1 \phi_2 + g_{13} n_1 \phi_3 \\ & + g_{14} n_1 \phi_4 + g_{23} n_2 \phi_3 + g_{24} n_2 \phi_4 \\ & + g_{34} n_3 \phi_4 \end{aligned} \quad (1)$$

where n_i is the number of moles, ϕ_i is the volume fraction of component i, g_{ij} is the interaction parameter between components i and j, R is the gas constant, and T is the absolute temperature. Subscripts 1–4 refer to the nonsolvent, solvent, first polymer, and second polymer, respectively. The effects of the polydispersity of polymer molecules are neglected. Following Flory's recommendation,[18] the number-average molecular weight is used for polymers.

When the proper derivatives of the Gibbs free energy of mixing are taken, the chemical potential of the mixing of component i($\Delta\mu_i$) may be written as

$$\begin{aligned}\Delta\mu_1/RT = {} & \ln \phi_1 - \phi_2(v_1/v_2) - \phi_3(v_1/v_3) \\ & - \phi_4(v_1/v_4) + (1 + g_{12}\phi_2 + g_{13}\phi_3 \\ & + g_{14}\phi_4)(1 - \phi_1) - g_{23}\phi_2\phi_3(v_1/v_2) \\ & - g_{34}\phi_3\phi_4(v_1/v_3) - g_{24}\phi_2\phi_4(v_1/v_2) \end{aligned} \quad (2)$$

$$\begin{aligned}\Delta\mu_2/RT = {} & \ln \phi_2 - \phi_1(v_2/v_1) - \phi_3(v_2/v_3) \\ & - \phi_4(v_2/v_4) + (1 + g_{12}\phi_1(v_2/v_1) + g_{23}\phi_3 \\ & + g_{24}\phi_4)(1 - \phi_2) - g_{13}\phi_1\phi_3(v_2/v_1) \\ & - g_{14}\phi_1\phi_4(v_2/v_1) - g_{34}\phi_3\phi_4(v_2/v_3) \end{aligned} \quad (3)$$

$$\begin{aligned}\Delta\mu_3/RT = {} & \ln \phi_3 - \phi_1(v_3/v_1) - \phi_2(v_3/v_2) \\ & - \phi_4(v_3/v_4) + (1 + g_{13}\phi_1(v_3/v_1) \\ & + g_{23}\phi_2(v_3/v_2) + g_{34}\phi_4)(1 - \phi_3) \\ & - g_{12}\phi_1\phi_2(v_3/v_1) - g_{14}\phi_1\phi_4(v_3/v_1) \\ & - g_{24}\phi_2\phi_4(v_3/v_2) \end{aligned} \quad (4)$$

$$\begin{aligned}\Delta\mu_4/RT = {} & \ln \phi_4 - \phi_1(v_4/v_1) - \phi_2(v_4/v_2) \\ & - \phi_3(v_4/v_3) + (1 + g_{14}\phi_1(v_4/v_1) \\ & + g_{24}\phi_2(v_4/v_2) + g_{34}\phi_3(v_4/v_3))(1 - \phi_4) \\ & - g_{12}\phi_1\phi_2(v_4/v_1) - g_{13}\phi_1\phi_3(v_4/v_1) \\ & - g_{23}\phi_2\phi_3(v_4/v_2) \end{aligned} \quad (5)$$

where v_i is the molar volume of component i. The conditions for an equilibrium between the two liquid phases I and II are

$$\Delta\mu_i^{\mathrm{I}} = \Delta\mu_i^{\mathrm{II}} \quad (i = 1, 2, 3, 4) \quad (6)$$

The material balance requires

$$\sum \phi_i^{\mathrm{I}} = \sum \phi_i^{\mathrm{II}} = 1 \quad (7)$$

Given a set of interaction parameters and temperature, six coupled nonlinear equations [eqs. (6) and (7)] can be solved for the individual tie lines of coexisting phases with the selection of two of the concentrations as independent variables. We selected ϕ_3^I and ϕ_4^I (volume fractions of two polymers in phase I) as independent variables with a constant ratio of ϕ_3^I and ϕ_4^I. The Newton–Raphson method based on a least-square procedure was employed to solve the simultaneous equations.[2,3,21]

To calculate the phase diagram numerically, a set of six interaction parameter values should be known at a given temperature. The following values relevant for a system consisting of water (1), NMP (2), PSF (3), and PES (4) were used in the calculations:

$$g_{12} = 1.4 \quad g_{13} = 2.7 \quad g_{14} = 1.6$$
$$g_{23} = 0.24 \quad g_{24} = 0.5 \quad g_{34} = 0.2$$

The g_{12} value was found to be concentration dependent.[15] Instead of the value of 1.0 used in other works,[15,21] a value of 1.4 was used considering the practical concentration range of the experiment.[14] The g_{13} and g_{14} values may be determined by the water sorption method,[2,15] and lower values were chosen for a reason similar to g_{12}.[14,15] The g_{23} and g_{24} values were from the literature.[14,15,20] The g_{34} value was measured in our laboratory as will be described later.

EXPERIMENTAL

Materials

PSF (Udel P-3500, M_n = 33500 g/mol and M_w = 50800 g/mol) from Amoco Performance Products and PES (Ultrason E6020P, M_n = 11,000 g/mol and M_w = 58,000 g/mol, porous flake) from BASF were used after sufficient drying. NMP (micropure electronic grade) from International Specialty Chemical was used as received. Water with an electrical resistance above 18 MΩ was used.

Cloud Point Measurement

Cloud points were determined by the titration of polymer solutions with water at various temperatures (20, 30, 45, and 60°C). Quantities of materials were determined by weight by using an electronic balance capable of reading up to 0.0001 g. For a polymer solution of 5 wt % or less, the solution viscosity was low enough to allow agitation by a magnetic bar. The flask was capped tightly with a rubber septum stopper to reduce solvent evaporation to a negligible amount. For solutions having more than 5 wt % polymer, mixing with a magnetic bar was not sufficient. A stainless steel stirring rod coated with Teflon was inserted through a Teflon cap with a rubber O ring.

The water was added to the clear polymer solution by a microsyringe through the septum until turbidity was observed. After turbidity was observed, the temperature of the bath that contained the sample flask was raised by 30°C above the titration temperature. If turbidity disappeared within several hours, the bath temperature was lowered to the titration temperature and more water was added. For the convenient thermal swing, a fast-acting thermostat bath was used.

Evaluation of PSF/PES Interaction Parameter

The thermodynamic interaction parameter between PSF and PES g_{34} can be expressed as follows[22]:

$$g_{34} = (\ln \phi_1 + (1 - \phi_1) + (g_{13}\phi_3 + g_{14}\phi_4)(1 - \phi_1))/\phi_3\phi_4 \quad (8)$$

where the ϕ_i values are the volume fraction of each component, and they can be obtained by the sorption experiment.

Films of PSF and PES were prepared by solution casting them on glass plates in weight ratios of 100/0, 80/20, 50/50, 20/80, and 0/100. For each blend ratio, samples (about 50 mm × 50 mm with a thickness of 80–100 μm) were weighed and immersed in distilled water at 20°C. They were weighed until no weight change was observed, and the volume fractions of each component at equilibrium were calculated.

RESULTS AND DISCUSSION

PSF/PES Interaction Parameter

The interaction parameter between PSF and PES was determined by a water sorption experiment. The g_{34} values were obtained in the range of −0.38 to 0.44 in various blend ratios. The measured interaction parameters of g_{34} are summarized in Table I.

Table I Interaction Parameters (g_{34}) for PSF-PES

PSF/PES (w/w)	g_{34}
20/80	0.44
50/50	−0.38
80/20	−0.09
Average	−0.01

For the calculation of the quaternary phase diagram, we tried several values in the range of −3.7 to 0.8; the value of 0.2 fit the experimental cloud point data better than other values. We also carried out a DSC experiment to obtain the glass transition temperature (T_g) of each polymer in the blends and were not able to find a clear shift of T_g in the whole blend ratio.

Experimental Cloud Points

The experimental phase diagrams of the quaternary system are shown in Figure 1 [a quaternary diagram in a tetrahedron in Fig. 1(a) and a pseudoternary diagram in which two polymers are lumped together in Fig. 1(b)]. The blend ratio of components 3 and 4 were kept constant.

Cloud point curves measured by the water titration experiments at 20°C showed unusual behavior as the blend ratio between PSF and PES was varied. In the triangular diagram of Figure 1(b), the cloud point curves of the solutions containing blends of PSF and PES do not fall in between that of pure PSF and pure PES. As the blend ratio between PSF and PES decreased from 100/0 (w/w), the cloud point curve went closer to the solvent–polymer edge. As the blend ratio decreased beyond a certain PSF/PES value of around 20/80 (w/w), the cloud point curve moved back toward the cloud point curve of PES. Considering the difference in the molecular weight of PSF (M_n = 33500) and PES (M_n = 11000), the critical composition in the binary blend of PSF and PES lies in the high PES range, which may be reflected in the quaternary diagram. It is very interesting to note that even with a 2/98 PSF/PES (w/w) composition, the phase separation occurred earlier with a small amount of water added compared to pure PES. The cloud points at low concentrations of polymer showed little shift toward the polymer–solvent edge as the blend ratio between PSF and PES was varied. However, the cloud points in the region having a higher concentration of polymer showed a significant move toward the edge. Figure 2 represents this behavior clearly.

Figure 2 shows the precipitation value (grams nonsolvent/100 g polymer solution to cause phase separation) of the cloud point titration experiment at 20°C for several polymer concentrations as a function of PES content in the polymer blend.

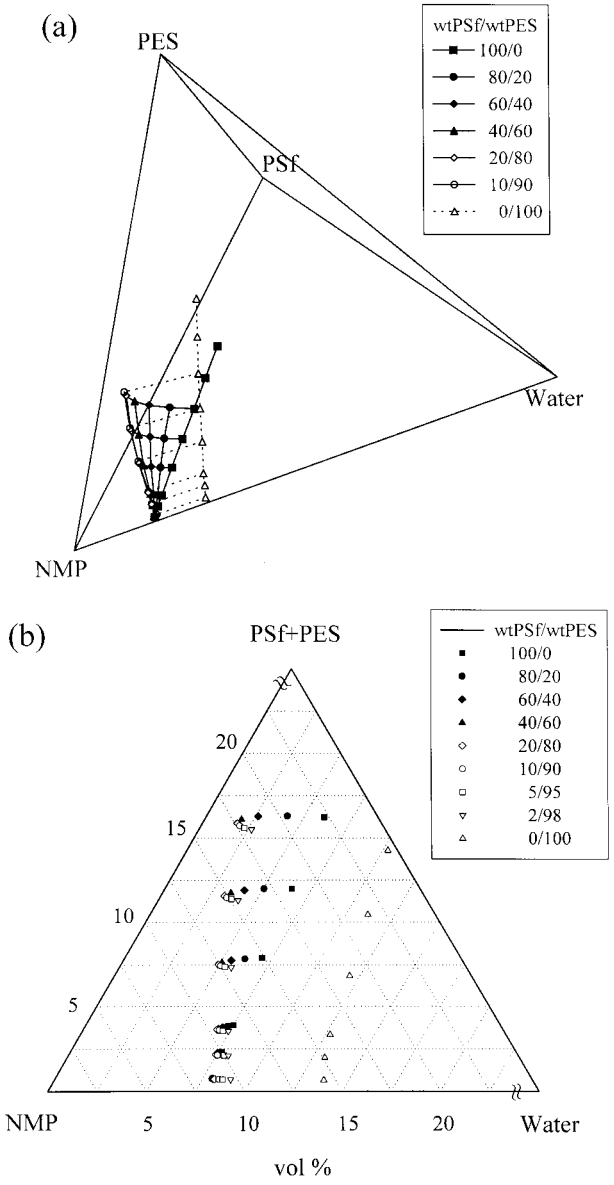

Figure 1 Experimental cloud points for the quaternary system of PSF/PES/NMP/water at 20°C with various weight ratios between the PSF and PES: (a) a quaternary phase diagram in a tetrahedron and (b) a pseudoternary phase diagram in which components PSF and PES were lumped together. The concentrations were converted into volume percents (vol %).

The precipitation value was almost constant up to the blend ratio of 2/98 PSF/PES (w/w), at which point the total polymer concentration was below 5 wt % but showed a minimum value around the blend ratio of 20/80 PSF/PES (w/w) when the total polymer concentration was above 5 wt %. Figures 1(b) and 2 indicate that the phase separation occurs with the addition of a smaller amount of nonsolvent (water) when the polymer solution contains the blend of PSF and PES and the miscible region in the solution of the blend is smaller than that of the pure PSF and the pure PES.

Calculated Phase Diagrams

As described in the earlier section, the binodal curves with a constant blend weight ratio of PSF and PES were calculated using the set of six interaction parameters. The calculated results are shown in a pseudoternary diagram rather than in a tetrahedron.[21] In Figures 3 and 4 components 3 and 4 are lumped together to give cross sections through the quaternary phase diagram in which the ratio of the concentrations of components 3 and 4 is kept constant. Although the incipient phases that are connected by the tie line do not fall into this cross section (in these phases, different ratios between components 3 and 4 exist), these compositions are projected onto the cross section. These phases represent the shadow curve as defined by Koningsveld and Straverman.[23]

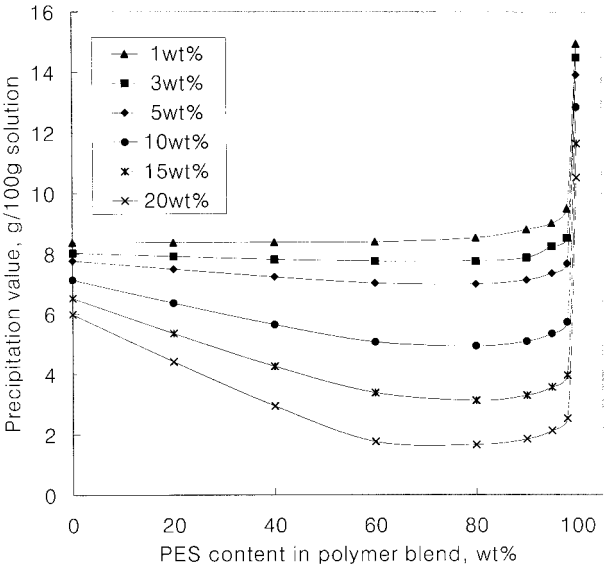

Figure 2 Precipitation values of water (grams water/100 g polymer solution) at 20°C as a function of the concentration of PES (wt %) in the polymer blends.

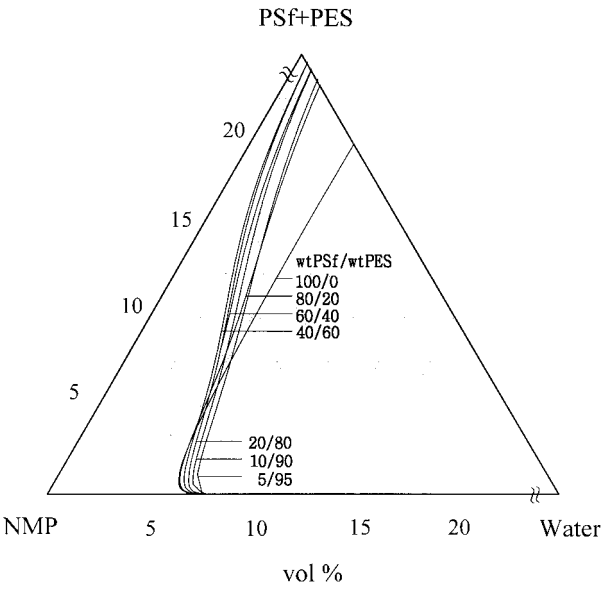

Figure 3 Calculated binodals for the PSF/PES/NMP/water quaternary system: the concentrations of components PSF and PES are lumped together with a constant weight ratio of PSF and PES. The concentrations were converted into volume percents (vol %).

When components 1 and 2 are lumped together in Figure 5, the binodal curve in the pseudoternary diagram leads to a straight line due to the assumed constant ratio of components 3 and 4. This type of diagram clearly demonstrates that the ratio of components 3 and 4 in the shadow curve connected by the tie line is different from that in the binodal curve.

The calculated binodal curves for the quaternary system are given in Figure 3 in comparison with the experimental cloud points of Figure 1(b). The miscible region is reduced in the solutions of the blend of PSF and PES compared to those of the pure PSF and PES, which is similar to the experimental results. Note that the calculated binodal curves fit the experimental cloud point curves well. However, the calculated phase diagram for the ternary system of water/NMP/PES did not match the experimental results; the water content to induce phase separation was above 25 vol % with the given values of interaction parameters, which is out of range in the graph of Figure 3.

In order to present the overall feature of the calculated phase diagram for the quaternary system of PSF/PES/NMP/water at 20°C, two types of pseudoternary diagrams are shown: PSF and PES in Figure 4 and water and NMP in Figure 5 for the PSF/PES blend ratios of 80/20, 40/60, 20/

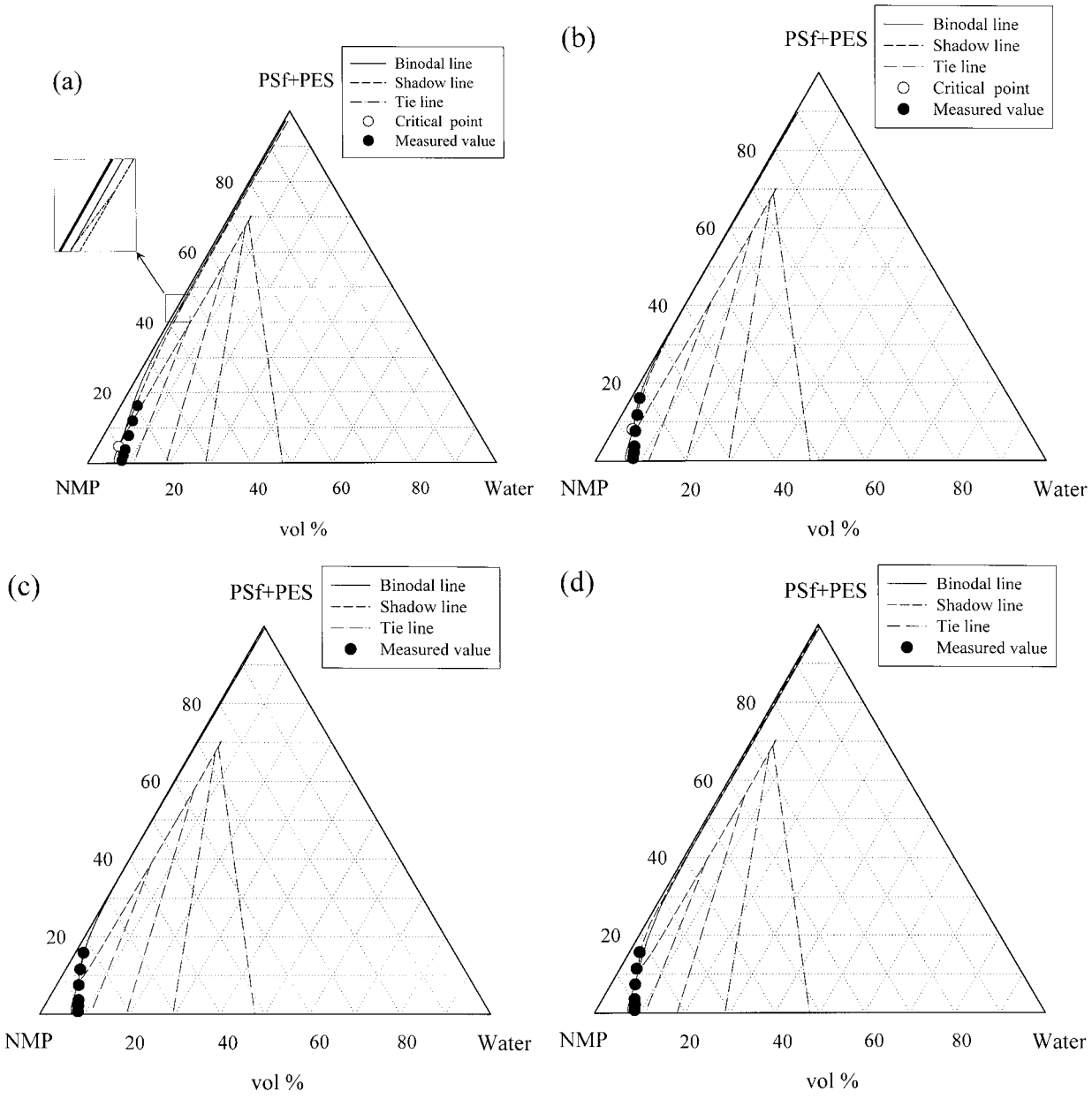

Figure 4 Comparison of experimental cloud points at 20°C with calculated phase diagrams for a constant weight ratio of the concentrations of PSF and PES: (a) 80/20 PSF/PES, (b) 40/60 PSF/PES, (c) 20/80 PSF/PES, and (d) 5/95 PSF/PES. The concentrations of PSF and PES are lumped together.

80, and 5/95 (w/w). The experimental cloud points are also included in Figure 4.

As can be seen in Figure 4(a), there are two shadow lines for the polymer-lean side and for the polymer-rich side that are joined at the critical point. The lower dashed line (shadow line) represents the polymer composition that is in equilibrium with a polymer-lean phase, which corresponds to a polymer–liquid phase separation. The upper dashed curve (shadow line) represents the polymer composition that is in equilibrium with another polymer-rich phase with the composition ratio of 80/20 PSF/PES (w/w), which corresponds to a polymer–polymer phase separation. This phenomenon can be seen more clearly in Figure 5(a), which is another form of phase diagram with the water and NMP components lumped together.

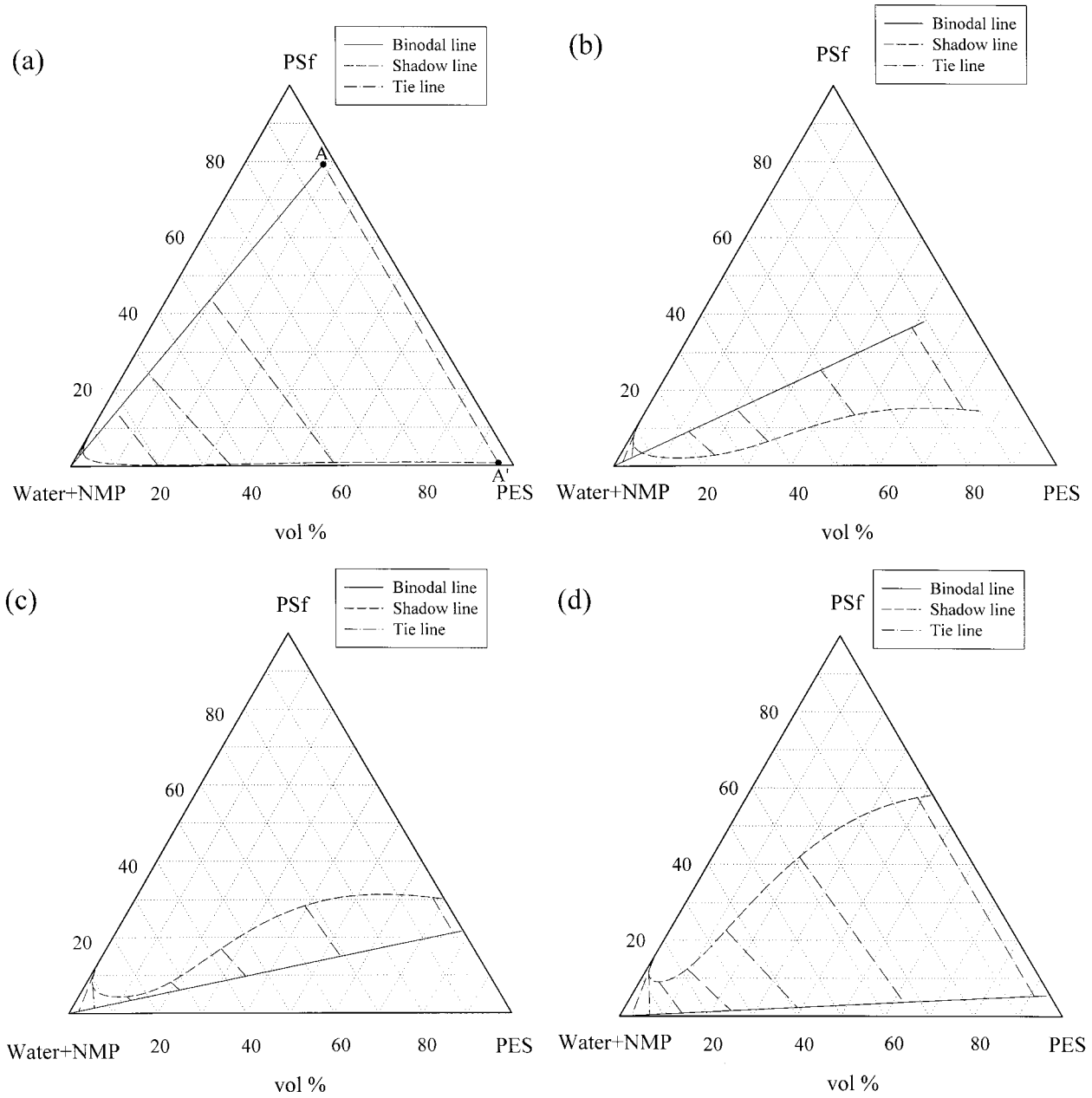

Figure 5 Pseudoternary plots of the calculated phase diagrams in which the concentrations of water and NMP are lumped together for a constant weight ratio of the concentrations of PSF and PES: (a) 80/20 PSF/PES, (b) 40/60 PSF/PES, (c) 20/80 PSF/PES, and (d) 5/95 PSF/PES.

The locus of the points where the binodal curve intersects the shadow curve represents the critical line in the quaternary system. The critical points on the critical line start from the low polymer concentration region below 10% [Fig. 5(a,b)] when the PSF/PES blend ratio is 80/20 or 40/60 (w/w). In the blend ratios of 20/80 and 5/95 [Fig. 5(c,d)] the critical point disappears. The composition where the critical point disappears was estimated to be about 25/75 PSF/PES (w/w) in our quaternary system. The disappearance of the critical point is ascribed to the assumed constant ratio of components 3 and 4 in calculation and depends on the values of the various molecular parameters used (molar volume ratios of each component and interaction parameters). For the

PES/poly(vinylpyrrolidone) (PVP)/water/NMP system reported by Boom et al. the value is about 30/70 PES/PVP (v/v) when the molecular weight of PVP is 1000 g/mol.[21] As shown in Figure 4(a,b), the location of the critical point shifts to higher total polymer concentration as the blend ratio decreases. Figure 4(a,b) indicates that when the total polymer concentration is above the critical point value, the solution shows polymer–polymer phase separation and when the total polymer concentration is below the critical point value the solution shows polymer–liquid phase separation.

Dual Mode of Phase Separation

The tie lines corresponding to the polymer–polymer phase separation are shown on the right side of the critical point in Figure 5(a). The phase corresponding to the binodal curve contains more PSF. The phase corresponding to the shadow line contains more PES. Thus, the compositions on the tie line are phase separated into a PSF-rich phase and a PES-rich phase. The tie lines corresponding to the polymer–liquid phase separation are shown on the right side in Figure 4(a) and on the left side of the critical point in Figure 5(a). The compositions connected by the tie line are phase separated into a polymer-rich phase and a polymer-lean phase.

In the ternary phase diagram of the solvent/nonsolvent/polymer system, the heterogeneous region may be separated into a metastable region and an unstable region. In the metastable region the nucleation and growth mechanism governs the phase separation. In the unstable region the spinodal decomposition mechanism governs the phase separation. For any point in the heterogeneous region, the composition is separated into a polymer-rich phase and a polymer-lean phase. In the quaternary system some compositions are separated into a polymer-rich phase and a polymer-lean phase (polymer–liquid separation). The other compositions in the heterogeneous region are separated into a polymer 1 rich phase and a polymer 2 rich phase (polymer–polymer separation).

The difference in these two types of phase separation was experimentally observed by adding water into the polymer solution of the initial 20 wt % total polymer concentration in vials. When a small amount of water was added, the solution remained homogeneous [group A in Fig. 6(a)]. Additional water caused phase separation of the solution and, after long periods of settling, two distinct layers developed. The sample of group B in Figure 6(a) shows two layers with similar viscosity. When the sample was inclined, the interface moved simultaneously with the top surface of the solution. In this sample the two layers are a polymer 1 rich phase and a polymer 2 rich phase (polymer–polymer separation). When more water was added to the solution, the phase-separated layers [group C in Fig. 6(a)] contained two layers

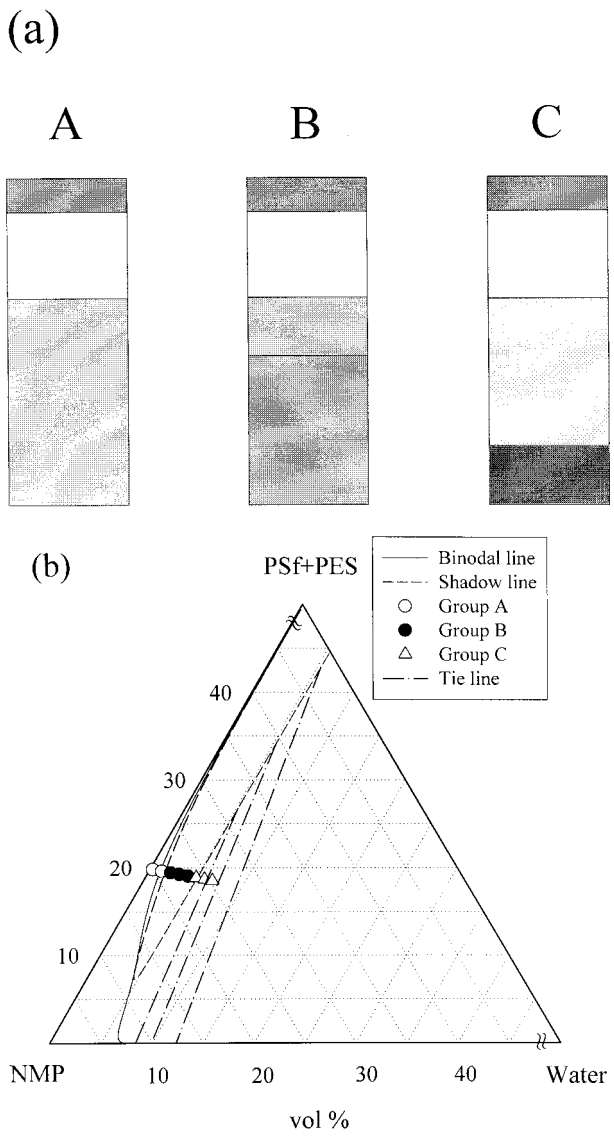

Figure 6 The dual mode of phase separation. (a) A schematic diagram of (○) group A, homogeneous state; (●) group B, polymer–polymer phase separation mode; and (△) group C, polymer–liquid phase separation mode. (b) The state of the samples of the initial 20 wt % total polymer concentration in the water addition experiment with the calculated phase diagram for a PSF/PES weight ratio of 40/60.

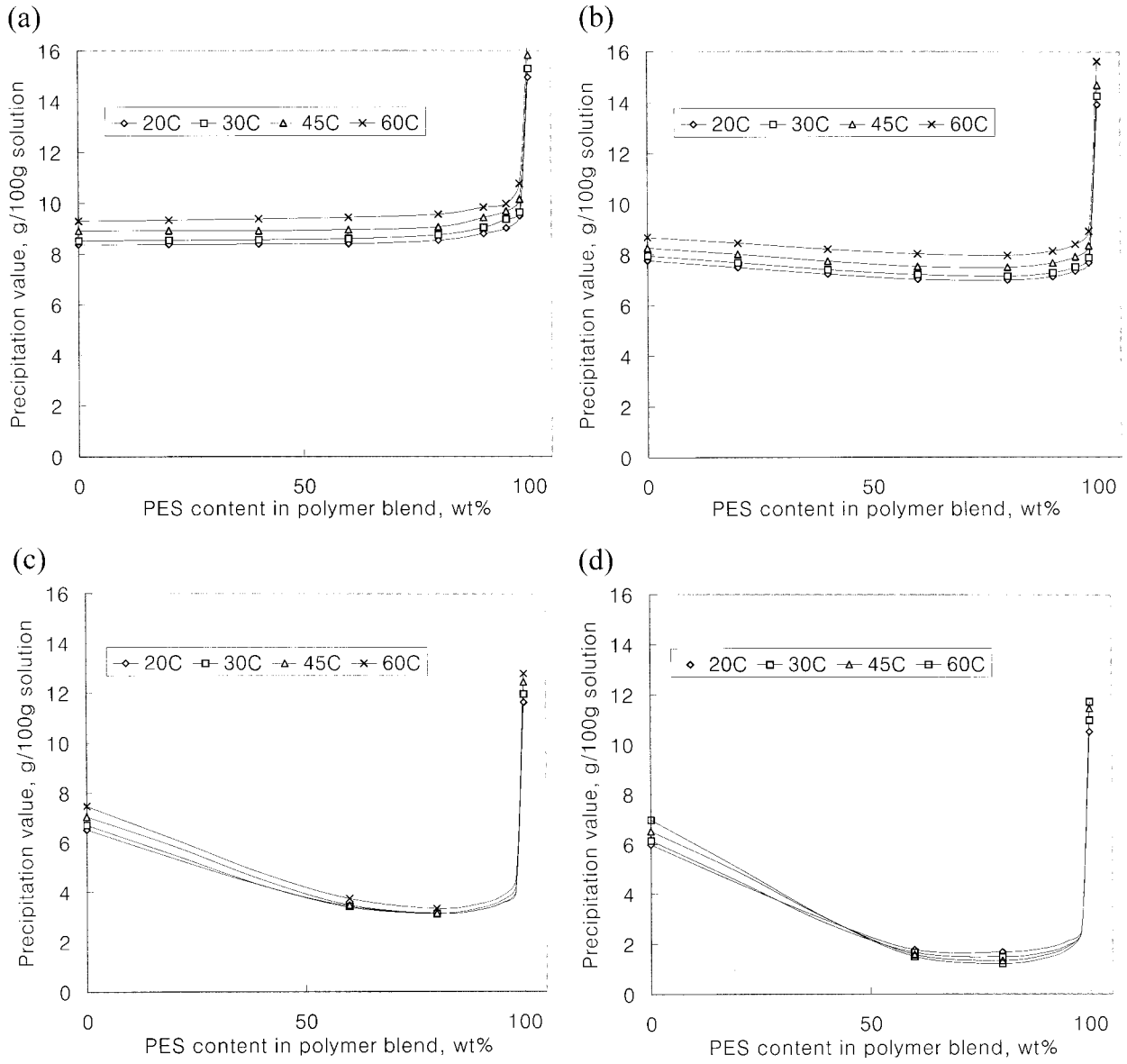

Figure 7 Precipitation values of water (grams of water/100 g of polymer solution) as a function of PES wt % in the polymer blend at various temperatures: (a) for 1 wt % of total polymer in solution, (b) for 5 wt % of total polymer in solution, (c) for 15 wt % of total polymer in solution, and (d) for 20 wt % of total polymer in solution.

having different viscosities. The upper layer flowed easily and the lower layer flowed very slowly when inclined. The difference in viscosity between the two layers seemed to be large. They had a polymer-rich phase and a polymer-lean phase (polymer–liquid separation). The results of the water addition experiment are shown in Figure 6(b). It was found that the boundary between the polymer–polymer separation and polymer–liquid separation was close to the lower shadow curve of the calculated phase diagram. These experimental results are consistent with the prediction by calculation.

The compositions in the locus of the tie lines connecting the lower binodal curve [defined as the binodal curve with total polymer concentrations less than the critical point value in Fig. 4(a,b)] and the corresponding shadow curve in the tetrahedron were separated into a polymer-rich phase and a polymer-lean phase (polymer–liquid separation). The compositions in the remaining heterogeneous region above the previously defined

polymer–liquid phase separation region were separated into a polymer 1 rich phase and a polymer 2 rich phase.

When the total polymer concentration is above the critical point value, one can easily see from the slopes of the tie lines in Figure 5(a,b) that the concentration of the total polymers in the PSF-rich phase is slightly lower than that in the PES-rich phase. When the polymer concentration is high, however, the total polymer concentration in each phase after phase separation is almost equal as shown in Figure 5(a) (tie line A–A′). The ratio of the concentrations of the two polymers in each phase is significantly different. This phenomenon appears in all blend ratios between the two polymers in Figure 5 when the total polymer concentration is higher than a certain value. Note that the critical point does not exist in Figure 5(c,d). Similar results were reported for the PES/PVP/NMP/water system.[21]

Effect of Temperature

The precipitation values at four different temperatures were determined in the polymer concentrations of 1, 3, 5, 10, 15, and 20 wt %. As shown in Figure 7, the difference of the precipitation values at different temperatures is relatively small, particularly for the 15 or 20 wt % of the total polymer concentration [Fig. 7(c,d)]. Interestingly, the lower critical solution temperature (LCST) behavior was observed in some regions. With a low concentration of total polymer (below 15 wt %), the precipitation value increased as the temperature increased. When the concentration of the total polymers was higher than 15 wt %, the precipitation values decreased as the temperature increased around the PSF/PES blend ratio range of 40/60 to 20/80 (w/w). For the PSF/PES blend ratio of 40/60 and 20/80 (w/w), the experimental cloud point curves are shown at 20 and 60°C in Figure 8. In order to examine this LCST phenomenon more clearly, 20 wt % total polymer solutions in NMP were kept at 20, 30, 45, and 60°C for the PSF/PES blend ratio of 40/60 (w/w). The solutions at 20 and 30°C were maintained as in the homogeneous state. However, the solutions at 45 and 60°C became hazy because of the phase separation.

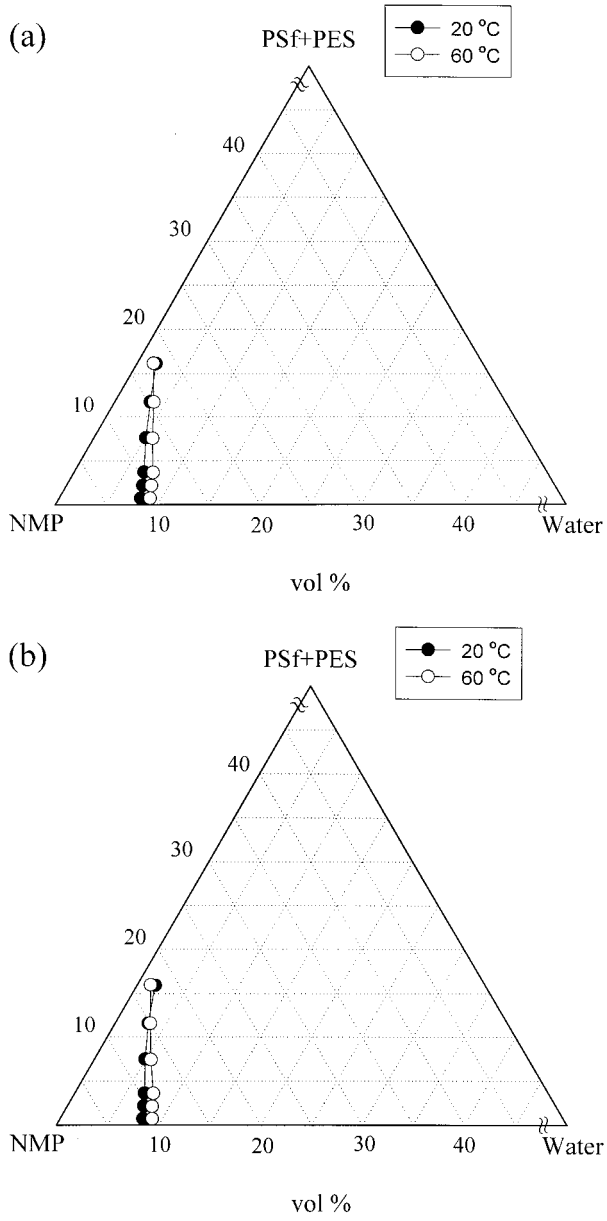

Figure 8 Experimental cloud points for the PSF/PES/NMP/water quaternary system in which components PSF and PES are lumped together at 20 and 60°C for (a) a constant PSF/PES weight ratio of 40/60 and (b) a constant PSF/PES weight ratio of 20/80. The concentrations were converted into volume percents (vol %).

CONCLUSIONS

Cloud points for the quaternary system of PSF/PES/NMP/water were determined by a titration method at 20, 30, 45, and 60°C. The cloud point curves of the solutions of the PSF and PES blends do not fall in between those of the pure PSF and PES solutions. The miscible region is narrowed when the blend of PSF and PES is used. The quaternary system showed two distinct types of phase separation: polymer-rich and polymer-lean phase separation (polymer–liquid separation) and PSF-rich and PES-rich phase separation (polymer–poly-

mer separation). The calculated binodal curves based on the Flory–Huggins theory fit the experimental cloud points well and the model appropriately described the phase separation behavior of the solution containing the blend of PSF and PES.

The LCST behavior was observed in some regions. When the total polymer concentration was higher than 15 wt %, the amount of water to initiate the phase separation of the polymer solution decreased with increasing temperature.

The interaction parameters between PSF and PES were obtained by water sorption experiments and had values ranging from -0.38 to 0.44, depending on the blend ratio. In the calculation of the quaternary phase diagram, the value of 0.2 as a constant parameter showed good agreement with the experimental cloud points.

REFERENCES

1. Mulder, M. H. V. Basic Principles of Membrane Technology; Elsevier: Amsterdam, 1991.
2. Altena, F. W.; Smolders, C. A. Macromolecules 1982, 15, 1491.
3. Yilmaz, L.; McHugh, A. J. J Appl Polym Sci 1986, 31, 997.
4. Kamide, K.; Matsuda, S.; Miyazaki, Y. Polym J 1984, 16, 479.
5. Cheng, L. P.; Dwan, A. H.; Gryte, C. C. J Polym Sci Part B Polym Phys 1994, 32, 1183.
6. Van de Witte, P.; Dijkstra, P. J.; Van den Berg, J. W. A.; Feijen, J. J Polym Sci Part B Polym Phys 1997, 35, 763.
7. Bulte, A. M. W.; Naafs, E. M.; van Eeten, F.; Mulder, M. H. V.; Smolders, C. A.; Strathmann, H. Polymer 1996, 37, 1647.
8. Staude, E.; Breitbach, L. J Appl Polym Sci 1991, 43, 559.
9. Tweddle, T. A.; Kutowy, O.; Thayer, W. L.; Sourirajan, S. Ind Eng Chem Prod Res Dev 1983, 22, 320.
10. Wijmans, J. G.; Kant, J.; Mulder, M. H. V.; Smolders, C. A. Polymer 1985, 26, 1539.
11. Swinyard, B. T.; Barrie, J. A. Br Polym J 1988, 20, 317.
12. Lau, W. W. Y.; Guiver, M. D.; Matsuura, T. J Membr Sci 1991, 59, 219.
13. Lau, W. W. Y.; Guiver, M. D.; Matsuura, T. J Appl Polym Sci 1991, 42, 3215.
14. Kim, J. Y.; Lee, H. K.; Baik, K. J.; Kim, S. C. J Appl Polym Sci 1997, 65, 2643.
15. Zeman, L.; Tkacik, G. J Membr Sci 1988, 36, 119.
16. Allen, G.; McAinsh, J.; Strazielle, C. Eur Polym J 1969, 5, 319.
17. Allen, G.; McAinsh, J. Eur Polym J 1970, 6, 1635.
18. Flory, P. J. Principles of Polymer Chemistry; Cornell University Press: Ithaca, NY, 1953.
19. Tompa, H. Polymer Solutions; Butterworths: London, 1956.
20. Boom, R. M.; Reinders, H. W.; Rolevink, H. H. W.; Van den Boomgaard, T.; Smolders, C. A. Macromolecules 1994, 27, 2041.
21. Boom, R. M.; Van den Boomgaard, T.; Smolders, C. A. Macromolecules 1994, 27, 2034.
22. Scott, R. L. J Chem Phys 1949, 17, 279.
23. Koningsveld, R.; Straverman, A. J. J Polym Sci Part A-2 1968, 2, 305.